Atmos. Chem. Phys., 13, 10659–10675, 2013
www.atmos-chem-phys.net/13/10659/2013/
doi:10.5194/acp-13-10659-2013

Atmospheric Chemistry and Physics Open Access

A global tropospheric ozone climatology from trajectory-mapped ozone soundings

G. Liu[1,*], J. Liu[2], D. W. Tarasick[1], V. E. Fioletov[1], J. J. Jin[3,], O. Moeini[3], X. Liu[4], C. E. Sioris[1], and M. Osman[1]**

[1]Air Quality Research Division, Environment Canada, 4905 Dufferin Street, Downsview, ON M3H 5T4, Canada
[2]Department of Geography and Program in Planning, University of Toronto, 100 St. George Street, Toronto, ON M5S 3G3, Canada
[3]Department of Earth and Space Science and Engineering, York University, Toronto, ON M3J 1P3, Canada
[4]Harvard-Smithsonian Center for Astrophysics, Cambridge, MA 21250, USA
[*]now at: Space Sciences Laboratory, University of California, Berkeley, CA, 94720, USA
[**]now at: GESTAR, Universities Space Research Association, Greenbelt, MD 20771, USA

Correspondence to: D. W. Tarasick (david.tarasick@ec.gc.ca)

Received: 11 February 2013 – Published in Atmos. Chem. Phys. Discuss.: 2 May 2013
Revised: 12 September 2013 – Accepted: 27 September 2013 – Published: 4 November 2013

Abstract. A global three-dimensional (i.e. latitude, longitude, altitude) climatology of tropospheric ozone is derived from the ozone sounding record by trajectory mapping. Approximately 52 000 ozonesonde profiles from more than 100 stations worldwide since 1965 are used. The small number of stations results in a sparse geographical distribution. Here, forward and backward trajectory calculations are performed for each sounding to map ozone measurements to a number of other locations, and so to fill in the spatial domain. This is possible because the lifetime of ozone in the troposphere is of the order of weeks. This physically based interpolation method offers obvious advantages over typical statistical interpolation methods. The trajectory-mapped ozone values show reasonable agreement, where they overlap, to the actual soundings, and the patterns produced separately by forward and backward trajectory calculations are similar. Major regional features of the tropospheric ozone distribution are clearly evident in the global maps. An interpolation algorithm based on spherical functions is further used for smoothing and to fill in remaining data gaps. The resulting three-dimensional global tropospheric ozone climatology facilitates visualization and comparison of different years, decades, and seasons, and offers some intriguing insights into the global variation of tropospheric ozone. It will be useful for climate and air quality model initialization and validation, and as an a priori climatology for satellite data retrievals. Further division of the climatology into decadal and annual averages can provide a global view of tropospheric ozone changes, although uncertainties with regard to the performance of older sonde types, as well as more recent variations in operating procedures, need to be taken into account.

1 Introduction

Ozone plays a major role in the chemical and radiative balance of the troposphere. Serving as a primary precursor to the formation of OH radicals, it controls the oxidizing capacity of the lower atmosphere, and thereby the capacity of the lower atmosphere to remove other pollutants. Ozone acts as an important infrared absorber (greenhouse gas), particularly in the upper troposphere, and because of multiple scattering, it is more effective in filtering surface UV-B than its small abundance in the troposphere (about 10 % of the total column) would suggest. However, at ground level, ozone is responsible for significant damage to forests and crops, and is a principal factor in air quality, as it has adverse effects on human respiratory health (Bell et al., 2004; Lippmann, 1991; McConnell et al., 2002; Jerret et al., 2009).

Balloon-borne ozonesondes are the major source of tropospheric ozone information at high vertical resolution (about 100 m for modern sondes). However, ozone soundings are limited in spatial and temporal coverage. Ozonesondes are normally released from ground stations at fixed locations.

Worldwide there are less than 100 stations that have routinely launched ozonesondes. These ozonesonde stations are generally located on continents and do not provide data over the oceans. Typically these stations launch sondes once a week, or at most 2–3 times a week, and as such temporal coverage is limited as well. Satellite observations of tropospheric ozone offer better spatial coverage, but are limited by the large stratospheric ozone burden that satellite instruments must look through (e.g. Bhartia, 2002). Recent instruments can provide some very limited vertical resolution, of about 6–10 km, in the troposphere (Worden et al., 2007a, b; X. Liu et al., 2005, 2010).

Several authors have developed ozone climatologies based entirely or partly on ozonesonde data (e.g. Logan, 1999; Fortuin and Kelder, 1998; Lamsal et al., 2004; McPeters et al., 1997, 2007; McPeters and Labow, 2012; Tilmes et al., 2012). A number of these have been used extensively in satellite ozone retrieval algorithms, which require an a priori estimate of the ozone profile (e.g. Bhartia, 2002), and as initial fields for climate models. With the exception of Tilmes et al. (2012), who considered aggregates of sonde data over a dozen large regions, all of these are zonally averaged (typically for 10° latitude bands), and thus lack longitudinal structure. This lack of horizontal resolution is a major limitation, and is of course owing to the geographic sparseness of the ozone sounding data record.

However, as the lifetime of ozone in the troposphere is of the order of weeks, a measurement of ozone mixing ratio at one place and time also provides a good estimate of ozone mixing ratio in that same air parcel several hours or days before and after. It is therefore possible to employ a technique that has been used successfully in the stratosphere (Sutton et al., 1994; Newman and Schoeberl, 1995; Morris et al., 2000) and use forward and backward trajectory calculations for each sounding to map ozone measurements to a number of other locations, and so to fill in the spatial domain. In the troposphere, trajectories have larger errors than in the stratosphere (Stohl and Seibert, 1998), primarily because of the importance of vertical motion, which is difficult to model accurately, but also because of turbulence in the boundary layer. Nevertheless, trajectory-based domain-filling models have been used successfully to extend ozone climatologies based on MOZAIC aircraft data (Stohl et al., 2001), to reconstruct tropospheric water vapour fields (Pierrehumbert, 1998; Pierrehumbert and Roca, 1998; Dessler and Minschwaner, 2007), and to analyse small-scale variations in ozone mixing ratio observed by research aircraft (Methven et al., 2003).

This technique has recently been employed successfully with tropospheric ozone profile data from the North American IONS ozonesonde intensive campaigns (Tarasick et al., 2010). Here we employ a similar technique to the global ozonesonde data set, using the entire World Ozone and Ultraviolet Radiation Data Centre (WOUDC) record, to produce an improved three-dimensional (latitude, longitude, altitude) tropospheric ozone climatology for the globe.

2 Ozonesonde data

All data employed in this study were obtained from the World Ozone and Ultraviolet Radiation Data Centre (WOUDC) (http://www.woudc.org/) from 116 ozonesonde stations worldwide. Their data spans are summarized in Table 1. The number of ozonesonde profiles available from different stations ranges from one to several thousand. Most of these stations are located in North America and Europe. There are only a few stations in Japan and along the east coast of China, giving somewhat poor coverage over Asia.

Most of the profiles are from the electrochemical concentration cell (ECC)-type ozonesonde, which was introduced in the early 1970s and adopted by the majority of stations in the global network by the early 1980s. Virtually all the data in the most recent decade are from ECC sondes. The remainder are from Brewer–Mast (BM) sondes (currently still in use at one site), the Japanese KC96 sonde, and the Indian sonde. Prior to the early 1990s, three stations in Europe (Praha, Lindenberg, and Legionowo) flew the GDR sonde. The majority of the data before 1980 is from BM sondes or similar (both the GDR and Indian sondes are similar in design to the BM sonde). A small amount of data is available from carbon–iodine sondes (similar to the KC sondes) and from Regener sondes (which operated by the chemiluminescent reaction of ozone with luminol) from the early 1960s.

When properly prepared and handled, electrochemical concentration cell (ECC) ozonesondes have a precision of 3–5 % (1σ) and an absolute accuracy of about 10 % in the troposphere (Smit et al., 2007; Kerr et al., 1994; Deshler et al., 2008; G. Liu et al., 2009). The ozone sensor response time (e^{-1}) of about 25 s gives the sonde a vertical resolution of about 100 m for a typical balloon ascent rate of $4\,\mathrm{m\,s^{-1}}$ in the troposphere. Two types of ECC ozonesondes are in current use – the 2Z model manufactured by EnSci Corp. and the 6A model manufactured by Science Pump, with minor differences in construction and some variation in recommended concentrations of the potassium iodide-sensing solution and of its phosphate buffer. The maximum variation in tropospheric response resulting from these differences is likely of the order of 2–3 % (Smit et al., 2007). Although in the past BM sondes have shown somewhat variable response in the troposphere depending on preparation (World Climate Research Programme, 1998; Kerr et al., 1994; Tarasick et al., 2002), recent intercomparisons show little bias in the troposphere and a precision of about 10 % (Smit et al., 1996). In early intercomparisons BM sondes showed negative biases of as much as 20 % (Attmannspacher and Dütsch, 1970; Hilsenrath et al., 1986). The Japanese KC series sondes show a precision of about 5 %, but a low bias in the troposphere of about 5 % (Smit and Straeter, 2004; Fujimoto et

Table 1. Ozonesonde stations used in this study and their respective data spans. (BM = Brewer–Mast; KC = Japanese KC series; CI = carbon–iodine).

WMO ID	Station Name	Station Latitude	Station Longitude	Altitude (m)	Sonde Type	Earliest Data	Latest Data	# of Profiles
18	ALERT/ALERT GAW LAB	82.49	−62.42	127	ECC	1987	2008	1122
21	EDMONTON/STONY PLAIN	53.55	−114.10	766	ECC	1978	2008	1286
76	GOOSE BAY	53.30	−60.36	40	ECC	1980	2008	1280
344	HONG KONG OBSERVATORY	22.31	114.17	66	ECC	2000	2008	361
43	LERWICK	60.13	−1.18	80	ECC	1992	2008	814
174	LINDENBERG	52.21	14.12	112	ECC	1992	2008	895
233	MARAMBIO	−64.23	−56.62	196	ECC	1988	2008	673
458	YARMOUTH	43.87	−66.10	9	ECC	2003	2008	231
316	DE BILT	52.10	5.18	4	ECC	1992	2008	860
29	MACQUARIE ISLAND	−54.50	158.97	6	ECC	1994	2008	554
308	MADRID / BARAJAS	40.46	−3.65	650	ECC	1994	2008	526
323	NEUMAYER	−70.65	−8.25	42	ECC	1992	2008	1258
107	WALLOPS ISLAND	37.90	−75.48	13	ECC	1970	2008	1636
156	PAYERNE	46.49	6.57	491	ECC	2002	2008	984
348	ANKARA	39.95	32.88	896	ECC	1994	2008	278
338	BRATTS LAKE (REGINA)	50.21	−104.71	592	ECC	2003	2008	271
457	KELOWNA	49.93	−119.40	456	ECC	2003	2008	281
24	RESOLUTE	74.72	−94.98	40	ECC	1978	2008	1101
53	UCCLE	50.80	4.35	100	ECC	1997	2008	1740
318	VALENTIA OBSERVATORY	51.93	−10.25	14	ECC	1994	2008	412
437	WATUKOSEK (JAVA)	−7.57	112.65	50	ECC	1999	2008	267
109	HILO	19.57	−155.05	11	ECC	1982	2008	1074
466	MAXARANGUAPE (SHADOZ-NATAL)	−5.45	−35.33	32	ECC	2002	2008	293
191	SAMOA	−14.25	−170.56	82	ECC	1995	2008	493
436	LA REUNION ISLAND	−20.99	55.48	68	ECC	1998	2008	282
256	LAUDER	−45.03	169.68	370	ECC	1986	2008	1384
494	ALAJUELA	9.98	−84.21	899	ECC	2007	2008	88
394	BROADMEADOWS	−37.69	144.95	108	ECC	1999	2008	433
435	PARAMARIBO	5.81	−55.21	23	ECC	1999	2008	437
443	SEPANG AIRPORT	2.73	101.70	17	ECC	1998	2008	322
77	CHURCHILL	58.75	−94.07	35	ECC	1978	2008	1193
450	DAVIS	−68.58	77.97	16	ECC	2003	2008	135
339	USHUAIA	−54.85	−68.31	15	ECC	2008	2008	30
315	EUREKA/EUREKA LAB	80.04	−86.18	310	ECC	1992	2008	1117
190	NAHA	26.20	127.68	27	ECC	2008	2008	3
175	NAIROBI	−1.27	36.80	1745	ECC	1996	2008	481
456	EGBERT	44.23	−79.78	253	ECC	2003	2008	221
221	LEGIONOWO	52.40	20.97	96	ECC	1993	2008	937
434	SAN CRISTOBAL	−0.92	−89.60	8	ECC	1998	2008	325
328	ASCENSION ISLAND	−7.98	−14.42	91	ECC	1990	2008	556
336	ISFAHAN	32.48	51.43	1550	ECC	1995	2008	120
242	PRAHA	50.02	14.45	304	ECC	1992	2008	818
418	HUNTSVILLE	34.72	−86.64	196	ECC	1999	2007	575
265	IRENE	−25.91	28.21	1524	ECC	1990	2007	365
477	HEREDIA	10.00	−84.11	1176	ECC	2006	2006	69
89	NY ALESUND	78.93	11.88	243	ECC	1990	2006	1711
262	SODANKYLA	67.34	26.51	179	ECC	1988	2006	1381
485	TECAMEC (UNAM)	19.33	−99.18	2272	ECC	2006	2006	35
361	HOLTVILLE (CA)	32.81	−115.42	−18	ECC	2006	2006	13
484	HOUSTON (TX)	29.72	−95.40	19	ECC	2004	2006	62
480	SABLE ISLAND	43.93	−60.02	4	ECC	2004	2006	61
260	TABLE MOUNTAIN (CA)	34.40	−117.70	2286	ECC	2006	2006	35
445	TRINIDAD HEAD	40.80	−124.16	55	ECC	1999	2006	197
490	VALPARAISO (IN)	41.50	−87.00	240	ECC	2006	2006	18
483	BARBADOS	13.16	−59.43	32	ECC	2006	2006	27
487	NARRAGANSETT	41.49	−71.42	21	ECC	2006	2006	44
488	PARADOX	43.92	−73.64	284	ECC	2006	2006	8
420	BELTSVILLE (MD)	39.02	−76.74	64	ECC	2006	2006	12
482	WALSINGHAM	42.60	−80.60	200	ECC	2006	2006	43
489	RICHLAND	46.20	−119.16	123	ECC	2006	2006	24
448	MALINDI	−2.99	40.19	−6	ECC	1999	2006	87
438	SUVA (FIJI)	−18.13	178.32	6	ECC	1997	2005	255
257	VANSCOY	52.12	−107.17	510	ECC	1990	2004	57
360	PELLSTON (MI)	45.56	−84.67	238	ECC	2004	2004	38
406	SCORESBYSUND	70.49	−21.98	50	ECC	1989	2003	647
460	THULE	76.53	−68.74	57	ECC	1991	2003	249
401	SANTA CRUZ	28.42	−16.26	36	ECC	1996	2003	322

Table 1. Continued.

WMO ID	Station Name	Station Latitude	Station Longitude	Altitude (m)	Sonde Type	Earliest Data	Latest Data	# of Profiles
95	TAIPEI	25.02	121.48	25	ECC	2000	2001	64
444	CHEJU	33.50	126.50	300	ECC	2001	2001	13
219	NATAL	−5.87	−35.20	32	ECC	1979	2000	219
432	PAPEETE (TAHITI)	−18.00	−149.00	2	ECC	1995	1999	168
439	KAASHIDHOO	5.00	73.50	1	ECC	1999	1999	54
254	LAVERTON	−37.87	144.75	21	ECC	1989	1999	275
404	JOKIOINEN	60.81	23.50	103	ECC	1995	1998	99
441	EASTER ISLAND	−27.17	−109.42	62	ECC	1995	1997	75
40	HAUTE PROVENCE	43.93	5.70	674	ECC	1981	1997	61
67	BOULDER	40.09	−105.25	1689	ECC	1979	1996	556
65	TORONTO	43.78	−79.47	198	ECC	1978	1994	8
297	S.PIETRO CAPOFIUME	44.65	11.62	11	ECC	1984	1993	98
333	PORTO NACIONAL	−10.80	−48.40	240	ECC	1992	1992	15
329	BRAZZAVILLE	−4.28	15.25	314	ECC	1990	1992	82
335	ETOSHA PAN	−19.20	15.90	1100	ECC	1992	1992	16
334	CUIABA	−15.60	−56.10	990	ECC	1992	1992	21
303	IQALUIT	63.75	−68.55	20	ECC	1991	1992	30
88	MIRNY	−66.55	93.00	30		1989	1991	114
280	NOVOLASAREVSKAYA/FORSTER	−70.77	11.87	110		1985	1991	393
111	AMUNDSEN-SCOTT (S Pole)	−89.98	0.00	2820		1967	1987	212
255	AINSWORTH (AIRPORT)	42.58	−100.00	789	ECC	1986	1986	7
228	GIMLI	50.63	−97.05	228	ECC	1980	1985	31
210	PALESTINE	31.80	−95.72	121	ECC	1975	1985	150
213	EL ARENOSILLO	37.10	−6.73	41	ECC	1983	1983	15
217	POKER FLAT	65.13	−147.45	358	ECC	1979	1982	40
198	COLD LAKE	54.78	−110.05	702	ECC	1979	1981	59
20	CARIBOU	46.87	−68.03	192	ECC	1981	1981	1
229	ALBROOK	8.98	−79.55	66	ECC	1980	1980	20
194	YORKTON	51.26	−102.47	504	ECC	1978	1978	10
203	FT. SHERMAN	9.33	−79.98	57	ECC	1977	1977	16
239	SAN DIEGO	32.76	−117.19	73	ECC	1977	1977	2
238	DENVER	39.77	−104.88	1611	ECC	1977	1977	1
237	GREAT FALLS	47.48	−111.35	1118	ECC	1977	1977	4
235	LONG VIEW	32.50	−94.75	103	ECC	1976	1976	2
236	COOLIDGE FIELD	17.28	−61.78	10	ECC	1976	1976	7
234	SAN JUAN	18.48	−66.13	17	ECC	1976	1976	6
231	SPOKANE	47.67	−117.42	576	ECC	1976	1976	7
224	CHILCA	−12.50	−76.80	−1	ECC	1975	1975	3
199	BARROW	71.32	−156.64	11	ECC	1974	1974	3
225	KOUROU	5.33	−52.65	4	ECC	1974	1974	3
227	MCDONALD OBSERVATORY	30.67	−90.93	2081	ECC	1969	1969	6
99	HOHENPEISSENBERG	47.80	11.02	975	BM	1966	2008	4362
156	PAYERNE	46.49	6.57	491	BM	1968	2002	3979
53	UCCLE	50.80	4.35	100	BM	1966	1997	3142
254	LAVERTON	−37.87	144.75	21	BM	1982	1990	134
213	EL ARENOSILLO	37.10	−6.73	41		1977	1983	20
197	BISCARROSSE/SMS	44.37	−1.23	18	BM	1976	1983	359
26	ASPENDALE	−38.03	145.10	1	BM	1965	1982	757
76	GOOSE BAY	53.30	−60.36	40	BM	1969	1980	532
38	CAGLIARI/ELMAS	39.25	9.05	4	BM	1968	1980	419
24	RESOLUTE	74.72	−94.98	40	BM	1966	1979	605
77	CHURCHILL	58.75	−94.07	35	BM	1973	1979	276
21	EDMONTON/STONY PLAIN	53.55	−114.10	766	BM	1970	1979	349
65	TORONTO	43.78	−79.47	198	BM	1976	1978	9
198	COLD LAKE	54.78	−110.05	702	BM	1977	1978	7
210	PALESTINE	31.80	−95.72	121	BM	1977	1977	13
194	YORKTON	51.26	−102.47	504	BM	1975	1977	62
104	BEDFORD	42.45	−71.27	80	BM	1969	1971	77
157	THALWIL	46.82	8.46	515	BM	1966	1968	187
67	BOULDER	40.09	−105.25	1689	BM	1963	1966	493
64	STERLING (WASHINGTON)	38.98	−77.48	84	BM	1963	1966	21
138	CHRISTCHURCH	−43.48	172.55	34	BM	1965	1965	25
101	SYOWA	−69.00	39.58	22	KC	1966	2008	1341
12	SAPPORO	43.06	141.33	19	KC	1969	2008	1039
14	TATENO / TSUKUBA	36.06	140.10	31	KC	1968	2008	1339
190	NAHA	26.20	127.68	27	KC	1989	2008	734
7	KAGOSHIMA	31.58	130.57	158	KC	1969	2005	841

Table 1. Continued.

WMO ID	Station Name	Station Latitude	Station Longitude	Altitude (m)	Sonde Type	Earliest Data	Latest Data	# of Profiles
437	WATUKOSEK (JAVA)	−7.57	112.65	50	KC	1998	1999	28
205	THIRUVANANTHAPURAM	8.48	76.97	60	Indian	1969	2008	226
187	PUNE	18.55	73.86	559	Indian	1966	2008	284
400	MAITRI	−70.46	11.45	224	Indian	1994	2008	141
10	NEW DELHI	28.49	77.16	248	Indian	1969	2007	265
206	BOMBAY	19.12	72.85	145	Indian	1968	1969	7
9	MOUNT ABU	24.60	72.70	1220	Indian	1965	1966	4
221	LEGIONOWO	52.40	20.97	96	GDR	1979	1993	497
174	LINDENBERG	52.21	14.12	112	GDR	1975	1992	1240
132	SOFIA	42.82	23.38	588	GDR	1982	1991	239
242	PRAHA	50.02	14.45	304	GDR	1979	1991	448
181	BERLIN/TEMPLEHOF	52.47	13.43	50	GDR	1966	1973	350
72	BYRD	−80.03	−119.52	1528	CI	1966	1966	11
111	AMUNDSEN-SCOTT (S POLE)	−89.98	0.00	2820	CI	1966	1966	8
64	STERLING (WASHINGTON)	38.98	−77.48	84	CI	1964	1966	41
105	FAIRBANKS (COLLEGE)	64.82	−147.87	138	CI	1965	1965	14
108	CANTON ISLAND	−2.76	−171.70	3	CI	1965	1965	4
53	UCCLE	50.80	4.35	100	Regener	1965	1966	14
64	STERLING (WASHINGTON)	38.98	−77.48	84	Regener	1962	1966	106
111	AMUNDSEN-SCOTT (S POLE)	−89.98	0.00	2820	Regener	1962	1966	103
72	BYRD	−80.03	−119.52	1528	Regener	1963	1965	100
109	HILO	19.57	−155.05	11	Regener	1964	1965	17
108	CANTON ISLAND	−2.76	−171.70	3	Regener	1965	1965	27
105	FAIRBANKS (COLLEGE)	64.82	−147.87	138	Regener	1964	1965	37
149	OVEJUYO (LA PAZ)	−16.52	−68.03	3420	Regener	1965	1965	10
131	PUERTO MONTT	−41.45	−72.83	5	Regener	1964	1965	7
76	GOOSE BAY	53.30	−60.36	40	Regener	1963	1963	49
69	HALLETT	−72.32	170.22	5	Regener	1962	1963	26
163	WILKES	−66.25	110.52	12	Regener	1963	1963	7
137	TOPEKA	39.07	−95.63	270	Regener	1963	1963	10

al., 2004; Kerr et al., 1994; Deshler et al., 2007). This bias appears to have been fairly consistent throughout the history of these sondes (Attmannspacher and Dütsch, 1970, 1981), but, like other sonde types, precision was poorer in the early period. In recent decades the Indian sonde has shown a precision of about 20 % (Kerr et al., 1994; Smit et al., 1996), with little bias, but in the period previous to this, precision was poorer and the sonde showed a positive bias in intercomparisons (Attmannspacher and Dütsch, 1970, 1981). The GDR sonde showed a negative bias in the lower troposphere of about 7 % and a positive bias, also of about 7 %, in the upper troposphere in two intercomparisons (Attmannspacher and Dütsch, 1970, 1981); however when only sondes with modest correction factors are considered, they show a much larger negative bias of about 20 % in the lower troposphere decreasing to about 5–10 % in the upper troposphere (Feister et al., 1985). During this earlier period both the Indian and the GDR sonde show significantly larger variability in tropospheric response than other sonde types. Regener sondes were used regularly for only a brief period in the 1960s, as they showed somewhat erratic response. Tropospheric response was also quite variable, with an average bias of about −40 % (Chatfield and Harrison, 1977; Hering and Dütsch, 1965).

No attempt has been made to correct for these biases, so the maps for the 1960s and the 1970s should be regarded as biased low. Data from the 1970s (Table 1) are primarily from Brewer–Mast sondes, which also seem to have been biased low in the troposphere, particularly at Canadian and Australian stations (Tarasick et al., 2002; Lehmann, 2005), but also probably in Europe (Attmannspacher and Dütsch, 1970, 1981; Hilsenrath et al., 1986). BM sondes show an increase in tropospheric response relative to ECC sondes between the 1970s and the early 1990s (Attmannspacher and Dütsch, 1970, 1981; Kerr et al., 1994; Smit et al., 2007). Improved preparation procedures for BM sondes (Attmannspacher and Dütsch, 1978; Claude et al., 1987; World Climate Research Programme, 1998) may have contributed to this, and there are indications that there have been some minor changes in sonde manufacture over the long period of record (World Climate Research Programme, 1998). ECC sondes have also changed since their introduction (there have been several models), and there is some evidence that they may have been biased high in the troposphere in the earlier period (Barnes et al., 1985; Hilsenrath et al., 1986), although the reasons for this are unclear. However, ECC data comprise less than 5 % of WOUDC ozonesonde data in the pre-1980 period. BM and GDR data comprise the bulk (81 %) of WOUDC ozonesonde data in the 1970s, while in the 1980s this fraction is 56 % (and 37 % for ECC sondes). This shift, in addition to the increase in BM sonde response during the 1970s and 1980s implied by the intercomparison data, may therefore cause an

apparent increase in tropospheric ozone. No attempt has been made to correct for this, but possible consequences are discussed below.

All ozonesonde data have been processed to 1 km altitude resolution. That is, ozone partial pressures are integrated and averaged for 1 km thick layers from sea level. Dividing by the average pressure in each layer gives values for average ozone mixing ratio. The altitude information for ozone is calculated using the hydrostatic relation from the pressure and temperature profiles measured by the coupled radiosonde. Ozone volume mixing ratio, which is treated as a conserved quantity following air parcel motions, can thus be calculated for each layer (altitude). The tropopause height was calculated for each profile according to the World Meteorological Organization (1992) criterion, that is, the lowest height at which the temperature lapse rate falls to $2\,^{\circ}\mathrm{C\,km^{-1}}$ or less, provided that the average lapse rate for 2 km above this height is also not more than $2\,^{\circ}\mathrm{C\,km^{-1}}$. Profiles without a defined tropopause were excluded. The layer containing the tropopause, as well as those above, was not used. No other data screening was employed; although comparison with a coincident total ozone measurement ("correction factor" screening) is often used as a measure of sonde data quality (e.g. Fioletov et al., 2006), it is not applicable to the tropospheric part of the profile, and would also reduce the number of available profiles. This was an important consideration given the relatively limited coverage of the data record. Data submitted to the WOUDC have already been processed and screened for quality by the station operator and can be expected to represent the station's best effort at accuracy. While some errors will undoubtedly escape detection, they are likely to be, at any rate, smaller than typical atmospheric variability (since they would otherwise be obvious), and therefore for the purpose of constructing this climatology, data with larger uncertainties are better than no data.

Correction factors, as the name suggests, have also been commonly used to scale sonde profiles to agree with a coincident total ozone measurement. There is evidence that this improves data quality (e.g. Kerr et al., 1994; Smit et al., 1996; Beekman et al., 1994, 1995; Fioletov et al., 2006) but also that it introduces additional uncertainty (Morris et al., 2013; Tarasick et al., 2005). Here too, there have been variations in practice between stations and over time. As for the larger issues discussed above, no attempt has been made to correct for these differences.

These practices are currently being re-evaluated and station data records homogenized under the Ozonesonde Data Quality Assessment activity of the SPARC/IGACO/IOC/NDAAC[1] initiative on "Past Changes in the Vertical Distribution of Ozone". Future versions of the climatology presented here may then use the re-evaluated data. The current version uses the data as they currently are found in the WOUDC.

3 Trajectory mapping

For each ozonesonde profile, at 1 km height intervals (0.5 km, 1.5 km, etc.) forward and backward trajectories were calculated using version 4.9 of the HYSPLIT model (Draxler and Hess, 1997, 1998), developed by the NOAA Air Resources Laboratory (NOAA ARL). The meteorological input for the trajectory model was the global NOAA-NCEP/NCAR (National Centers for Environmental Prediction/National Center for Atmospheric Research) pressure level reanalysis data set. An air parcel was assumed to be released at each 1 km altitude (above sea level) from the ozonesonde station (the releasing time, latitude, and longitude were taken from the ozonesonde launch). Four days of both backward and forward trajectories were calculated for the air parcel movement, and the original (1 km altitude resolution) ozone data were mapped to the locations calculated for every six hours along the forward and backward trajectory paths. In this way each original data value was mapped into 32 additional ozone mixing ratio values. The original and trajectory-mapped data were then binned at intervals of 5° latitude and 5° longitude, at each 1 km altitude, and averaged. This bin size corresponds to the typical ozone correlation length in the troposphere of about 500 km (G. Liu et al., 2009). Two different altitude coordinates were employed for this binning, and so two sets of maps were produced, one whose vertical coordinate is altitude above sea level, and the other altitude above ground level. Both sets of maps are presented with and without smoothing.

Figure 1 illustrates the improved spatial coverage if trajectory mapping is used. The plots shown are for ozone integrated between 0 and 1 km above the surface and for 5 to 6 km above sea level. Different ages of trajectories are indicated by different colours. Figure 1 demonstrates that the trajectory mapping greatly spreads out the ozone information along the trajectory paths, increasing the spatial domain to include most of the globe within 3–4 days. Coverage is excellent, especially above the planetary boundary layer (PBL).

The reliability of the information thus obtained depends upon the accuracy of the calculated trajectories, and also on the assumption that ozone chemistry can be neglected over a 4-day timescale. The latter assumption is generally valid, since the average lifetime of ozone is about 22 days in the troposphere (Stevenson et al., 2006), although it varies with latitude, altitude, and season. In particular, it is less in the boundary layer and in the tropics (von Kuhlmann et al., 2003; Roelofs and Lelieveld, 1997). Moreover, as is well known, in pollution plumes photochemistry can produce ozone on

[1] SPARC = Stratosphere-troposphere Processes And their Role in Climate
IOC = International Ozone Commission
IGACO = Integrated Global Atmospheric Chemistry Observations
NDACC = Network for the Detection of Atmospheric Composition Change

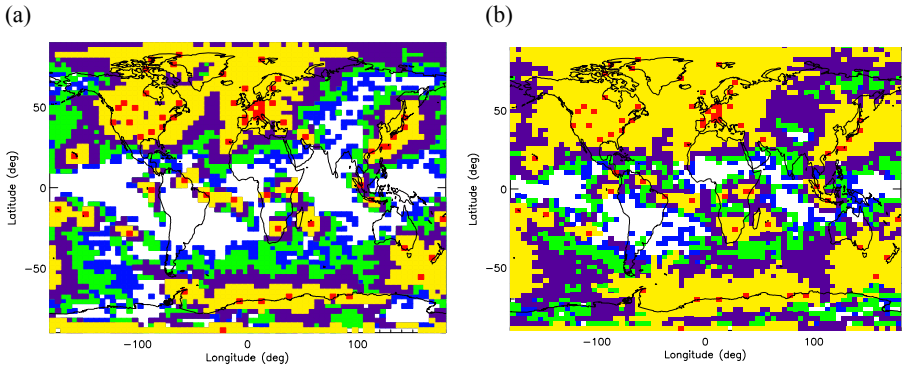

Fig. 1. Spatial coverage of 1-day (yellow squares), 2-day (purple squares), 3-day (green squares), and 4-day (blue squares) trajectories in April for **(a)** 0.5 km altitude above the surface **(b)** 5.5 km above sea level. The red squares denote the actual locations of the ozonesonde stations.

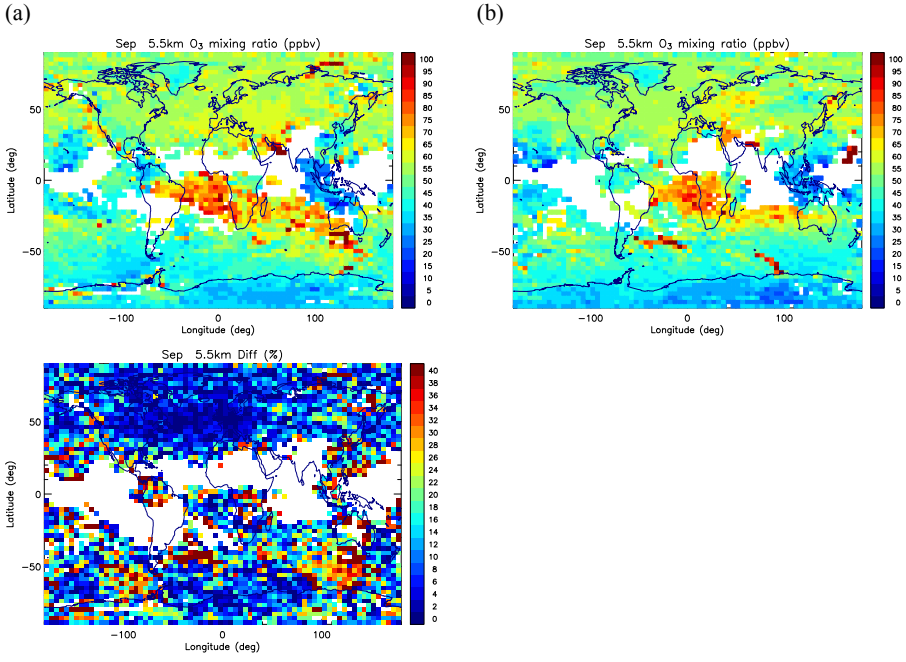

Fig. 2. Ozone distribution at 5.5 km from forward **(a)** and backward **(b)** trajectory mapping. **(c)** Difference between the two distributions in percent. Data from 1980 to 2008 are used.

timescales of a few days (e.g. Mao et al., 2006; Palmer et al., 2013), and lightning can produce ozone both directly (Minschwaner et al., 2008) and via lightning-generated NOx (e.g. Morris et al., 2010; Cooper et al., 2006), so this assumption can be violated in certain circumstances.

A number of studies have attempted to estimate, through several different methods, the accuracy of trajectories. Downey et al. (1990) estimated typical errors of 350 km for 4-day trajectories based on estimated wind errors. Stohl (1998) gave a comprehensive review of studies using balloons, material tracers, smoke plumes, and Saharan dust to evaluate trajectory errors, and quoted typical errors of 20 % of the trajectory distance, or about 100–200 km day^{-1} (with wide variation between studies). More recently Harris et al. (2005) evaluated trajectory model sensitivity to uncertainties in input meteorological fields and found uncertainties of 30–40 % of the horizontal trajectory distance, or 600–1000 km after four days, while Engström and Magnusson (2009), using an ensemble analysis method, found typical errors in the Northern Hemisphere of 350–400 km after three days, and $\sim$ 600 km after four days.

Sub-grid-scale convective processes are also not captured by HYSPLIT trajectories, which are calculated from gridded meteorological analysis fields. Convection is generally sporadic and randomly distributed, and its neglect does not likely represent an important bias to the average horizontal

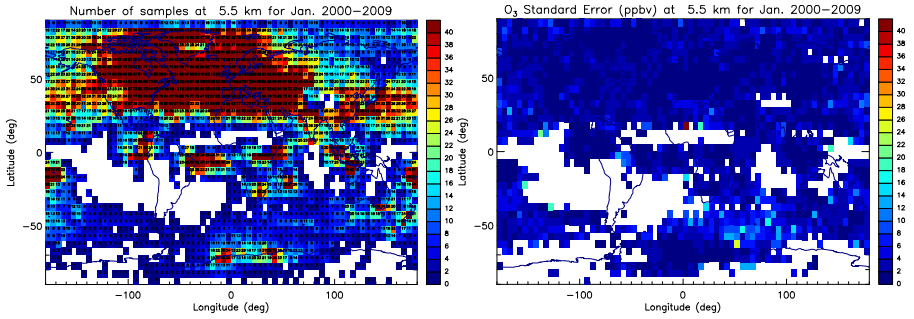

Fig. 3. Number of data values and the standard error of the mean for each pixel average in a decadal average map for January in the mid-troposphere. The standard errors are generally of the order of a few ppbv (right figure), although where data density is low (left figure), they can be higher.

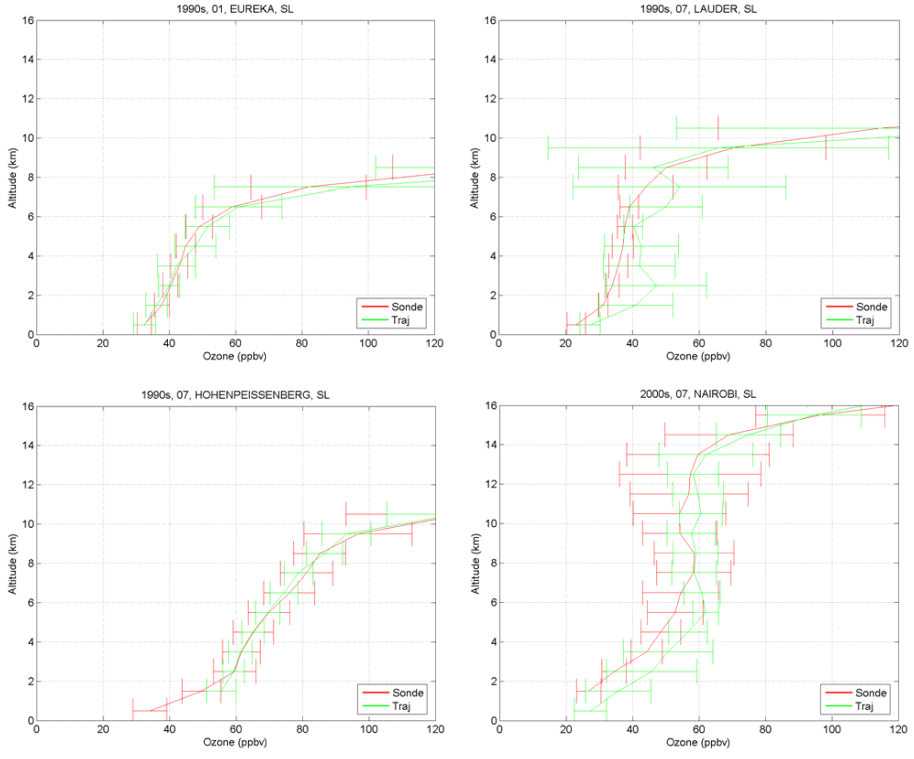

Fig. 4. Comparisons between the monthly (01 = January; 07 = July) averaged measured ozonesonde profiles and trajectory-mapped fields, for several sites. "Sonde" is the ensemble of measured profiles for that site; "Traj" is the profile generated from the mapping procedure when data from that site is omitted. Error bars indicate 2-σ confidence levels. The vertical coordinate is altitude from sea level (SL).

transport of ozone, except possibly in the Intertropical Convergence Zone. However, it is an important mechanism for the vertical mixing of ozone, and so acts to reduce vertical gradients; vertical gradients in this climatology might therefore be biased high, although not so much as to be evident in the validation comparisons. On a larger scale, the NCEP reanalysis apparently overestimates the convective precipitation in the tropics and in summer over Europe and North America (Stendel and Arpe, 1997), and this is presumably reflected as a bias in the vertical motion fields.

The estimates of ~ 100–$200\,\mathrm{km\,day^{-1}}$ quoted above represent errors for individual trajectories in the troposphere. Errors in the final product should be much reduced by averaging of multiple trajectories, at least to the extent that single trajectory errors are random. However, in the PBL, complex dispersion and turbulence tends to render single trajectories less representative of the actual flow (Stohl and Seibert, 1998), and several authors suggest using an ensemble of trajectories (Merrill et al., 1985; Stohl, 1998). In the PBL, therefore, the averaging of ozone values from multiple

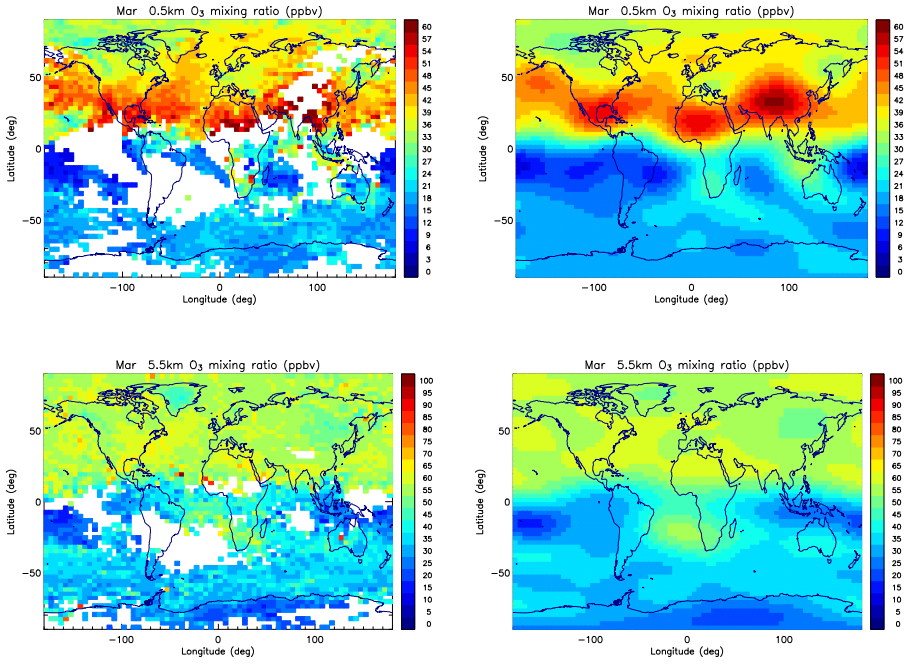

Fig. 5. Ozone maps at 0.5 km altitude above the surface and 5.5 km above sea level. Left-hand side: mapping; right-hand side: after smoothing and interpolation. Data from 1980 to 2008 are used.

trajectories in each pixel, as well as subsequent horizontal averaging (smoothing), will be particularly important for reducing trajectory errors. We nevertheless expect results for the lowest (0–1 km) layer to be less accurate than for higher levels. The ozone lifetime is also generally shorter near the surface, especially over the continents where dry deposition is a major loss process, affecting the validity of the assumption that chemistry can neglected.

Figure 2 assesses the differences between the ozone mapping produced using only backward and only forward trajectories. If ozone chemistry (i.e. local production in polluted regions) were a significant source of error, then one would expect to see differences between these maps. However, the ozone distribution patterns are in fact very similar. Differences have been calculated for all altitude levels, months, and latitude regions. Differences are most commonly 10 % or less, and found to be less than 40 % for almost all cases. As Fig. 2c illustrates, differences also show no distinct pattern except for some clustering in areas where the trajectories are longest, and therefore least reliable. As differences between the two distributions are comparable with the uncertainties of the mean values estimates and not systematic, it is reasonable to combine forward- and backward-mapped ozone values to produce an averaged ozone map.

The choice of September for these figures and April for those previous is arbitrary. The complete climatology comprises more than 15 000 maps, and we have tried to show a variety of examples in the few figures in this paper.

Figure 3 shows the number of data values and the standard error of the mean for each pixel average in a typical decadal map. The standard errors are generally of the order of a few ppbv, although where data density is low, they can be higher. Note that this is for a 10 yr average; for the 30 yr averages, corresponding errors are smaller.

A revealing test of an interpolation model is to examine how it performs in areas where no data are available. Figure 4 compares ozone profiles produced via trajectory mapping with actual measured profiles for several ozonesonde stations. For this comparison the mapping uses ozonesonde measurements from all sites except the one being compared, and combines both forward and backward trajectories. Agreement is generally quite good in the free troposphere, with some larger differences in the lowest layer and near the tropopause. The differences near the surface might be expected since, as noted earlier, trajectories are probably less accurate in the PBL and photochemical production and loss of ozone is more rapid there. In the tropopause region ozone concentrations increase rapidly (and dynamic variability is large). Note that differences are shown in absolute units (ppbv).

Similar comparisons of mapped profiles with MOZAIC (aircraft) ozone profile data also show very good agreement (Tarasick et al., 2010). Maps for the 0–1 km layer over North America show reasonable agreement with maps of mean daily 1 h maximum surface ozone from the National Air Pollution Surveillance (NAPS) network Canada-wide database and the US EPA Air Quality System (AQS)

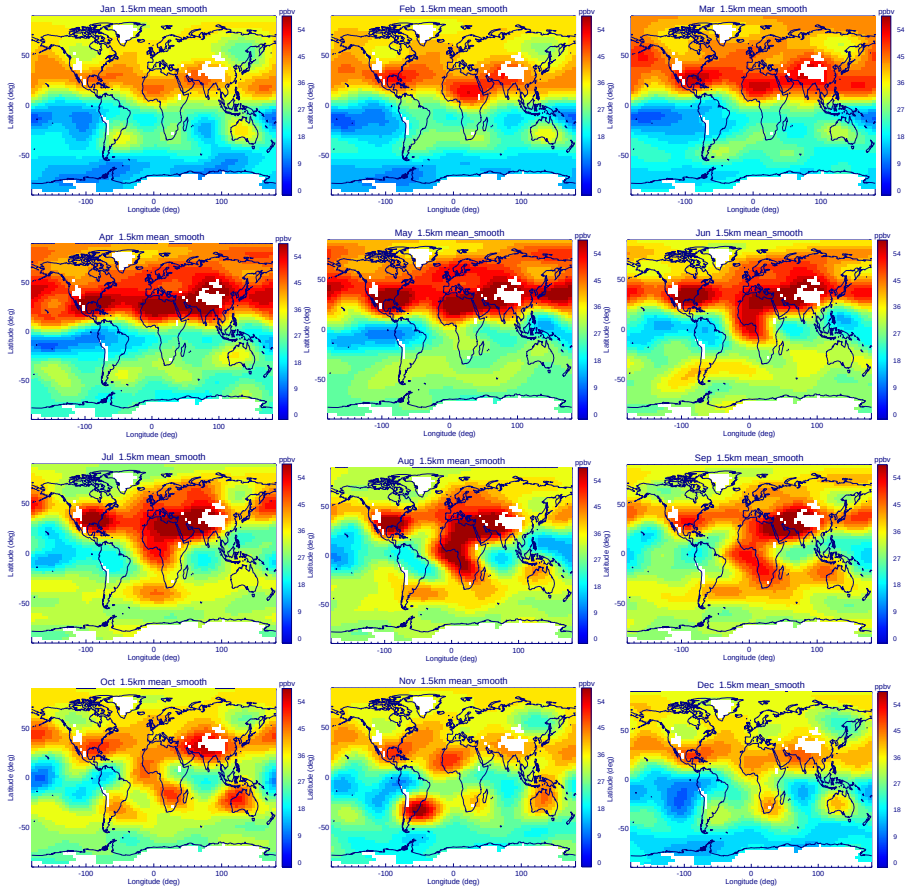

Fig. 6. Global ozone distributions at 1.5 km above sea level for all months. The trajectory-mapped results have been smoothed and further interpolated. Data from 1980 to 2008 are used.

database (1160 sites total), with correlation coefficients generally between 0.6 and 0.7 (Tarasick et al., 2010).

Figure 1 indicates that although the 4-day trajectory mapping greatly expands the spatial coverage of the ozonesonde measurements, there are still places where no ozone measurement is available. In order to fill in these data gaps and reduce small-scale "noise", the climatological average values obtained from the mapping are fitted to a linear combination of spherical functions. Figure 5 compares the ozone maps that are obtained from the trajectory mapping directly and following interpolation and smoothing by the spherical function interpolation algorithm. For a given altitude and month, the interpolated maps resemble the original maps, retaining broad features while reducing small-scale variability. In March, at the 0–1 km altitude level (above the surface), there are four strong ozone peaks in the northern extratropics. Three of these peaks are centred on the continents, while the remaining peak is over the Pacific Ocean. A similar pattern is seen at 5.5 km (above sea level), with weaker amplitudes and without the peak over the Himalayas (as this feature in the surface map is due to the high terrain). Similar features are seen in the tropospheric ozone column (TOC) fields produced from OMI/MLS observations (Ziemke et al., 2006; see http://acdb-ext.gsfc.nasa.gov/Data_services/cloud_slice/gif/cl1.gif, although the TOC fields show low values over the Himalayas, the Andes, and the Rocky Mountains, since the atmospheric column is much less there due to the high terrain. Low values are of course also seen in the TOC fields calculated by vertically integrating the fields in this climatology (not shown).

The original and interpolated maps have been compared for all months and altitude levels (not shown) in order to evaluate the impact of the smoothing. Typical differences (for individual pixels) are similar to those found for the forward/backward trajectory comparisons: about 10–30 % in the tropics and in the southern mid-latitude region, and about 10–20 % in northern mid-latitudes.

Figure 6 shows the smoothed ozone fields at 1.5 km altitude above the surface for each month, while Fig. 7 shows the same fields at 4.5 km above sea level. Taken together, these again reproduce (as they should) features seen in the tropospheric ozone column (TOC) fields from OMI/MLS (with the exception of the low values over mountainous regions). Well-known features such as the continental outflow from North

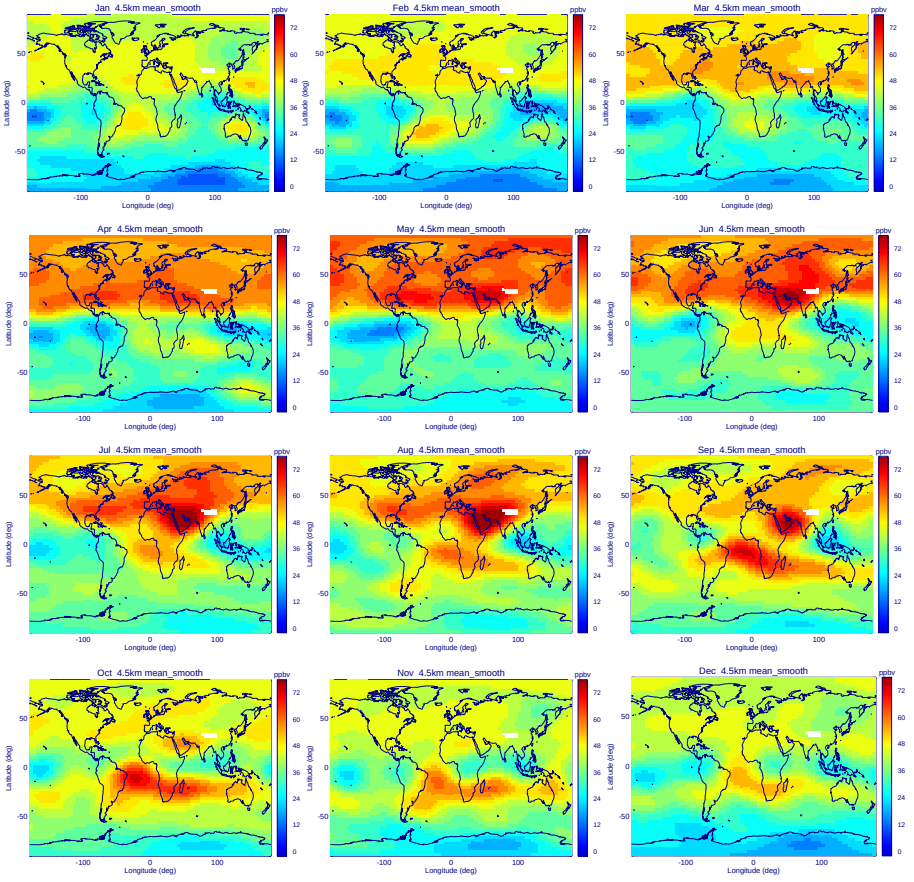

Fig. 7. As Fig. 6 but for 4.5 km altitude above sea level.

America, the summer ozone buildup over the Middle East (e.g. J. Liu et al., 2009), and biomass burning in the Southern Hemisphere, are clearly visible. The ozone production hotspots of the Middle East/Asia and the southern US are the most evident features, particularly in Fig. 6, but others – such as the continental outflow from the southeastern US, noted in satellite observations two decades ago (Fishman et al., 1990), and the influence of biomass burning in southern Africa and Indonesia – are also clearly visible. Interestingly, comparison of Figs. 6 and 7 shows that there are strong differences in the degree to which these emissions are lofted. Those from South America are much more evident at 4.5 km (Fig. 7) over the South Atlantic, especially in October, while burning in Australia's Northern Territory is much more evident nearer the surface (Fig. 6). Also, at 4.5 km, the global ozone hotspot is the Middle East in summer, while northern and equatorial Africa show the highest ozone values nearer the surface. Both these features have been previously reported: the former has been observed in TES data (J. Liu et al., 2009), while the latter has been seen in MOZAIC data (Sauvage et al., 2005).

Figure 6 also shows the global variation in the seasonal cycle of tropospheric ozone. Ozone at 1–2 km is highest in the summer over the US, northern Africa, the Middle East, and much of Europe and southern Asia, as well as over equatorial Africa and the southern oceans. In contrast, over Canada, the northern oceans and everywhere in the Arctic and sub-Arctic, ozone peaks in the March-April-May season, while over South America, southern Africa, and Australia the maximum occurs in the September-October-November season. This is quite consistent with recent model studies (Royal Society, 2008; see Box 5.2), although Fig. 6 shows little evidence of an equatorial maximum in the December-January-February season, as is predicted there.

Figures 8 and 9 show unsmoothed monthly maps at 4–5 and at 1–2 km for January and July for each decade since 1970. The lack of tropical data is evident in the pre-SHADOZ decades. Most notable, however, is the lack of evident change between decades after 1980. Some increase is apparent from the 1970s to the 1980s, but the patterns are remarkably similar in the following decades (although the patterns are smoother as the data density is greater). Figure 10 makes this more quantitative: a detailed comparison of the decadal data for all months, averaging over all $5^\circ \times 5^\circ$ pixels on the global map for which there is data for all four decades, produces several curves for the ratio of ozone concentration with altitude. The curves for the 1980s and 1990s indicate

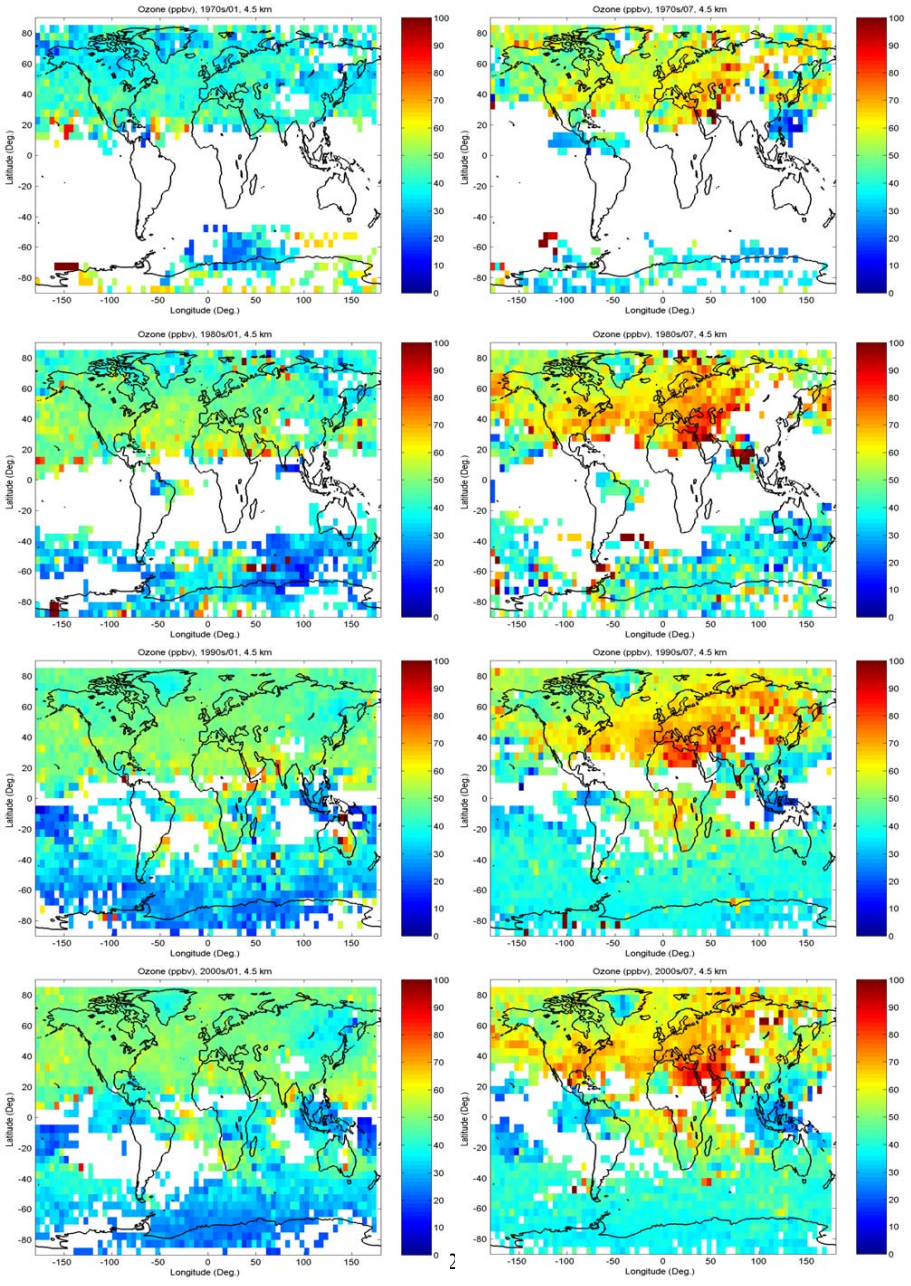

Fig. 8. Unsmoothed ($5° \times 5°$ pixel averaged) maps at 4–5 km, for January (01) and July (07), for each decade since 1970.

that over the area of complete sampling, average tropospheric ozone was about 1–3 % lower in the lowest 2 km of the troposphere in the 1980s and 1990s than in the 2000s, while above 2 km it was 1–4 % lower in the 1990s and 1–3 % higher in the 1980s. This quasi-global average change is generally consistent with the results of the recent detailed trend study of Oltmans et al. (2012), but somewhat smaller than the trends found by Parrish et al. (2012) and Cooper et al. (2010).

The corresponding curve for the 1970s suggests a large increase below about 6–7 km. However, as discussed above, recent comparisons show good agreement between ECC and BM sondes (e.g. Stubi et al., 2008), but past intercomparisons show a low bias for BM (and GDR) sondes. Such historical biases, and in combination with the migration of the global network to ECC sondes, may account at least in part for the post-1970 change. In fact, the curve for the 1970s closely resembles the corrections suggested for older BM data (Tarasick et al., 2002; Lehmann, 2005; Attmannspacher and Dütsch, 1970, 1981; Hilsenrath et al., 1986).

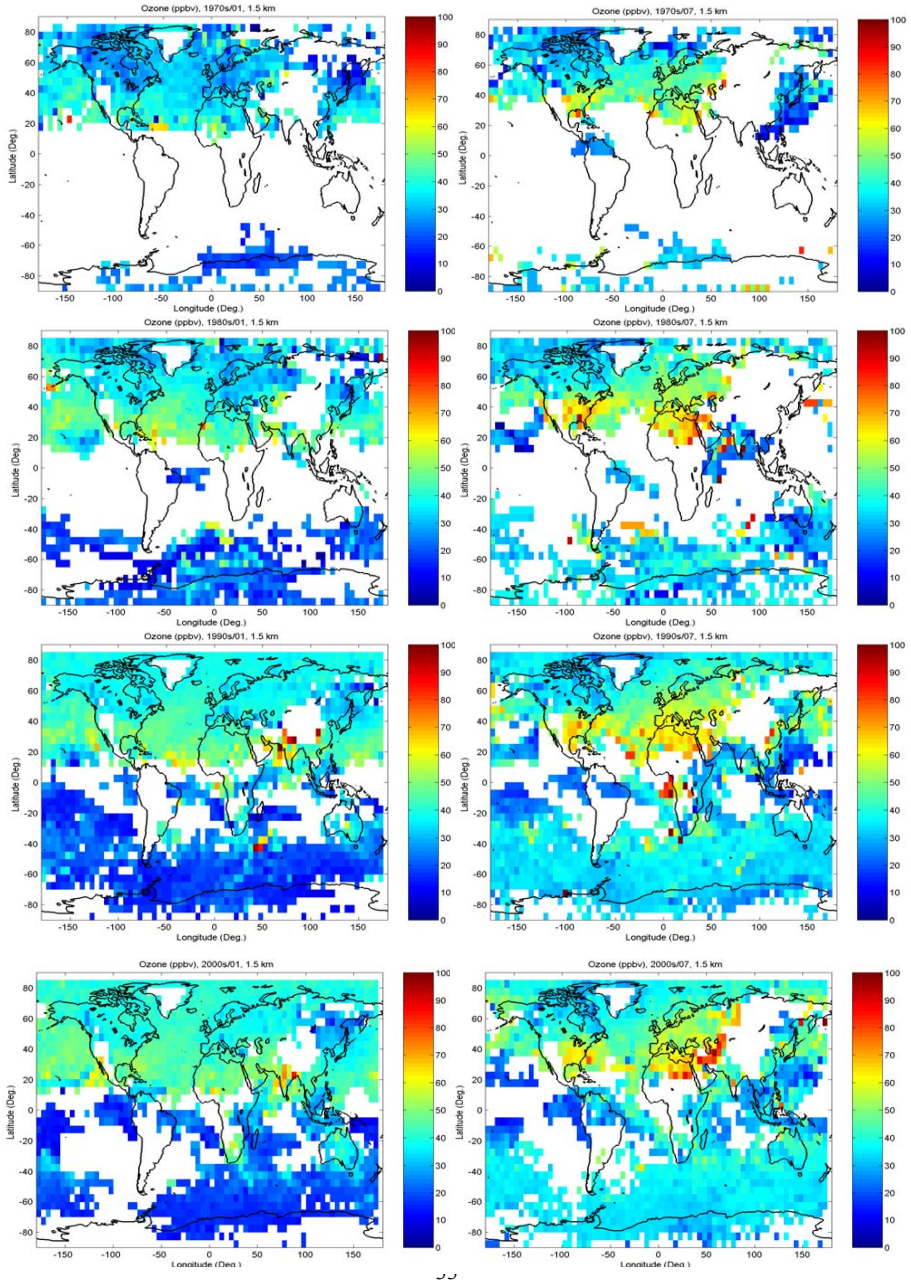

Fig. 9. Unsmoothed ($5^\circ \times 5^\circ$ pixel averaged) maps at 1–2 km for January (01) and July (07) for each decade since 1970.

4 Conclusions

A spatial domain-filling technique using forward and backward trajectory calculations applied to the large sets of ozone soundings in the WOUDC has been shown to produce self-consistent maps of the global ozone distribution for each month and altitude level in the troposphere from the 1960s to the 2000s. An interpolation method based on spherical functions is used for smoothing and to fill any remaining data gaps.

The mapped profiles agree well with sounding data excluded from the mapping, and maps produced using only backward and only forward trajectories also show good agreement (usually within 10 %, and almost always within 40 %). The resultant three-dimensional ozone fields show features that, where they have significant vertical extent, are also seen in tropospheric ozone column fields derived from OMI/MLS measurements.

The ozone climatology maps thus obtained exhibit many previously noted features of the seasonal distribution of ozone in the troposphere, while providing a wealth of detail

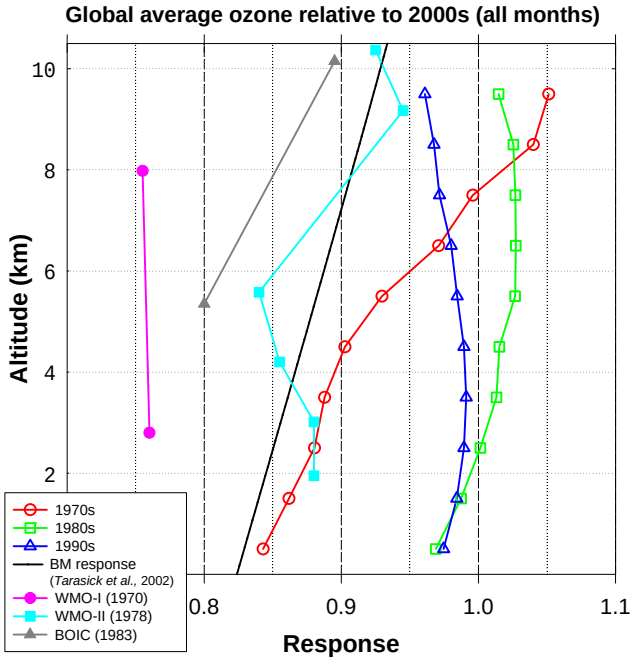

Fig. 10. Decadal average tropospheric ozone as a function of altitude, compared to the most recent decade. Averages are over all $5° \times 5°$ pixels on the global map for which there is data for all four decades. Also shown for reference are a quadratic best fit to BM response data from Tarasick et al. (2002), the average difference between BM and ECC response from ozonesonde intercomparisons in 1970 and 1978 (Attmannspacher and Dütsch, 1970, 1981), and the average response of BM sondes with respect to a reference UV photometer on the same balloon in 1983 (Hilsenrath et al., 1986).

about its horizontal and vertical variation. This detailed global picture offers some intriguing insights, such as the global variation in the seasonal cycle of tropospheric ozone, and a global view of tropospheric ozone changes over four decades.

It is expected that this climatology will be useful to other researchers as background information for (aircraft and model) process studies and for initialization and validation of models. It will also be useful for satellite data retrievals, which often require an accurate a priori profile of the vertical distribution of ozone in order to derive accurate column ozone amounts, to compensate for the lack of sensitivity to the lower troposphere, or to constrain profile retrieval algorithms. The TOC fields, obtained by integrating the climatology to the climatological average tropopause height, may also be used for validation of TOC retrievals.

Although not discussed here, by combining months, it is possible to produce maps of annual averages with similar data coverage. This technique offers the ability to map ozone near globally with high vertical resolution in the lower troposphere. Satellite remote sensing currently cannot provide such a product. These annual averages, or the seasonally resolved decadal averages, may be particularly valuable for validation of model studies of both recent tropospheric ozone changes (e.g. Jonson et al., 2006) and longer-term changes (e.g. Young et al., 2013).

Maps and data files are available from the authors and may also be downloaded at http://www.woudc.org.

Acknowledgements. The authors thank the many observers who, over many years, obtained the ozonesonde measurements used in this study. Their careful work is gratefully acknowledged. The global ozone sounding data were obtained from the World Ozone and Ultraviolet Radiation Data Centre (WOUDC, http://www.woudc.org) operated by Environment Canada, Toronto, Ontario, Canada, under the auspices of the World Meteorological Organization. We also gratefully acknowledge the the NOAA Air Resources Laboratory (ARL) for the provision of the trajectory model HYSPLIT (Hybrid Single Particle Lagrangian Integrated Trajectory Model) (http://www.arl.noaa.gov/ready.html), and the NOAA Physical Sciences Division for the NCEP/NCAR reanalysis data (http://www.esrl.noaa.gov/psd/data/reanalysis/reanalysis.shtml).

Edited by: A. Dastoor

References

Attmannspacher, A. and Dütsch, H. U.: International ozone sonde intercomparison at the Observatory Hohenpeissenberg, Ber. Dtsch. Wetterdienstes, 120, 1–85, 1970.

Attmannspacher, A. and Dütsch, H. U.: Second international ozone sonde intercomparison at the Observatory Hohenpeissenberg, Ber. Dtsch. Wetterdienstes, 157, 1–64, 1981.

Barnes, R. A., Bandy, A. R., and Torres, A. L.: Electrochemical concentration cell ozonesonde accuracy and precision, J. Geophys. Res., 90, 7881–7887, doi:10.1029/JD090iD05p07881, 1985.

Beekman, M., Ancellet, G., Mégie, G., Smit, H. G. J., and Kley, D.: Intercomparison campaign of vertical ozone profiles including electrochemical sondes of ECC and Brewer-Mast type and a ground-based UV-differential absorption lidar, J. Atmos. Chem., 19, 259–288, 1994.

Beekman, M., Ancellet, G., Martin, D., Abonnel, C., Duverneuil, G., Eideliman, F., Bessemoulin, P., Fritz, N., and Girard, E.: Intercomparison of tropospheric ozone profiles obtained by electrochemical sondes, a ground-based lidar and an airborne UV-photometer, Atmos. Environ., 29, 1027–1042, 1995.

Bell, M. L., McDermott, A., Zeger, S. L., Samet, J. M., and Dominici, F.: Ozone and short-term mortality in 95 US urban communities, 1987–2000, JAMA-J. Am. Med. Assoc., 292, 2372–2378, 2004.

Bhartia, P. K.: "OMI Algorithm Theoretical Basis Document: Volume II, OMI Ozone Products", ATBD-OMI-02, Version 2.0, August 2002.

Chatfield, R. and Harrison, H.: Tropospheric ozone: 1. Evidence for higher background values, J. Geophys. Res., 82, 5965–5968, doi:10.1029/JC082i037p05965, 1977.

Claude, H., Hartmannsgruber, R. and Köhler, U.: Measurement of Atmospheric Profiles using the Brewer-Mast Sonde, WMO Global Ozone Research and Monitoring Project, Report No. 17, 1987.

Cooper, O. R., Stohl, A., Trainer, M., Thompson, A., Witte, J. C., Oltmans, S. J., Johnson, B. J., Merrill, J., Moody, J. L., Morris, G., Tarasick, D., Forbes, G., Nédélec, P., Fehsenfeld, F. C., Meagher, J., Newchurch, M. J., Schmidlin, F. J., Turquety, S., Crawford, J. H., Pickering, K. E., Cohen, R. C., Bertram, T., Wooldridge, P., and Brune, W. H.: Large upper tropospheric ozone enhancements above mid-latitude North America during summer: In situ evidence from the IONS and MOZAIC ozone monitoring network, J. Geophys. Res., 111, D24S05, doi:10.1029/2006JD007306, 2006.

Cooper, O. R., Parrish, D. D., Stohl, A., Trainer, M., Nédélec, P., Thouret, V.,. Cammas, J. P, Oltmans, S. J., Johnson, B. J., Tarasick, D., LeBlanc, T., McDermid, I. S., Jaffe, D., Gao, R., Stith, J., Ryerson, T., Aikin, K., Campos, T., and Weinheimer, A.: Increasing springtime ozone mixing ratios in the free troposphere over western North America, Nature, 463, 344–348, doi:10.1038/nature08708, 2010.

Deshler, T., Mercer, J., Smit, H. G. J., Stuebi, R., Levrat, G., Johnson, B. J., Oltmans, S. J., Kivi, R., Thompson, A. M., Witte, J., Davies, J., Schmidlin, F. J., Brothers, G., and Sasaki, T.: Atmospheric comparison of electrochemical cell ozonesondes from different manufacturers, and with different cathode solution strengths: The Balloon Experiment on Standards for Ozonesondes, J. Geophys. Res., 113, D04307, doi:10.1029/2007JD008975, 2008.

Dessler, A. E. and Minschwaner, K.: An analysis of the regulation of tropical tropospheric water vapor, J. Geophys. Res., 112, D10120, doi:10.1029/2006JD007683, 2007.

Downey, A., Jasper, J. D., Gras, J., and Whittlestone, S.: Lower tropospheric transport over the Southern Ocean, J. Atmos. Chem., 11, 43–68, doi:10.1007/BF00053667, 1990.

Draxler, R. R. and Hess, G. D.: An overview of the HYSPLIT_ 4 modelling system for trajectories, dispersion and deposition, Aust. Meteorol. Mag., 47, 295–308, 1998.

Draxler, R. R. and Hess, G. D.: Description of the HYSPLIT_ 4 modeling system, NOAA Technical Memorandum ERL ARL-224, December, 24 pp., 1997.

Engström, A. and Magnusson, L.: Estimating trajectory uncertainties due to flow dependent errors in the atmospheric analysis, Atmos. Chem. Phys., 9, 8857–8867, doi:10.5194/acp-9-8857-2009, 2009.

Feister, U., Grasnick, K. H., and Peters, G.: Performance of the electrochemical ozone sonde OSR, Pure Appl. Geophys., 123, 422–440, 1985.

Fioletov, V. E., Tarasick, D. W., and Petropavlovskikh, I.: Estimating ozone variability and instrument uncertainties from SBUV(/2), ozonesonde, Umkehr and SAGE II measurements. Part 1: Short-term variations, J. Geophys. Res., 111, D02305, doi:10.1029/2005JD006340, 2006.

Fishman, J., Watson, C. E., Larsen, J. C., and Logan, J. A.: Distribution of tropospheric ozone determined from satellite data, J. Geophys. Res., 95, 3599–3617, doi:10.1029/JD095iD04p03599, 1990.

Fortuin, J. and Kelder, H.: An ozone climatology based on ozonesonde and satellite measurements, J. Geophys. Res., 103, 31709–31733, 1998.

Fujimoto, T., Sato, T., Nagai, K., Nakano, T., Shitamichi, M., Kamata, Y., Miyauchi, S., Akagi, K., and Sasaki, T.: Further evaluation and improvements of Japanese KC-Ozonesonde through JOSIE-2000, Proc. XX Quadrennial Ozone Symposium, 1–8 June 2004, Kos, Greece, International Ozone Commission, Athens, 540–541, 2004.

Harris, J. M., Draxler, R. R., and Oltmans, S. J.: Trajectory model sensitivity to differences in input data and vertical transport method, J. Geophys. Res., 110, D14109, doi:10.1029/2004JD005750, 2005.

Hering, W. S. and Dütsch, H. U.: Comparison of chemiluminescent and electrochemical ozonesonde observations, J. Geophys. Res., 70, 5483–5490, doi:10.1029/JZ070i022p05483, 1965.

Hilsenrath, E., Attmannspacher, W., Bass, A., Evans, W., Hagemeyer, R., Barnes, R. A., Komhyr, W., Mauersberger, K., Mentall, J., Proffitt, M., Robbins, D., Taylor, S., Torres A., and Weinstock, E.: Results from the balloon intercomparison campaign (BOIC), J. Geophys. Res., 91, 13137–13152, 1986.

Jerrett, M., Burnett, R. T., Pope III, C. A., Ito, K., Thurston, G., Krewski, D., Shi, Y., Calle, E., and Thun, M.: Long-Term Ozone Exposure and Mortality, N. Engl. J. Med., 360, 1085–1095, 2009.

Jonson, J. E., Simpson, D., Fagerli, H., and Solberg, S.: Can we explain the trends in European ozone levels?, Atmos. Chem. Phys., 6, 51–66, doi:10.5194/acp-6-51-2006, 2006.

Kerr, J. B., Fast, H., McElroy, C. T., Oltmans, S. J., Lathrop, J. A., Kyro, E., Paukkunen, A., Claude, H., Köhler, U., Sreedharan, C. R., Takao, T., and Tsukagoshi, Y.: The 1991 WMO international ozonesonde intercomparison at Vanscoy, Canada, Atmos.-Ocean, 32, 685–716, 1994.

Lamsal, L., Weber, M., Tellmann, S., and Burrows, J.: Ozone column classified climatology of ozone and temperature profiles based on ozonesonde and satellite data, J. Geophys. Res., 109, D20304, doi:10.1029/2004JD004680, 2004.

Lehmann, P.: An Estimate of the Vertical Ozone Profile Discrepancy between the Australian Brewer – Mast and Electrochemical Concentration Cell Ozonesondes, J. Atmos. Ocean. Tech., 22, 1864–1874, doi:10.1175/JTECH1821.1, 2005.

Lippmann, M.: Health-effects of tropospheric ozone, Envir. Sci. Tech., 25, 1954–1962, 1991.

Liu, G., Tarasick, D. W., Fioletov, V. E., Sioris, C. E., and Rochon, Y. J.: Ozone correlation lengths and measurement uncertainties from analysis of historical ozonesonde data in North America and Europe, J. Geophys. Res., 114, D04112, doi:10.1029/2008JD010576, 2009.

Liu, J. J., Jones, D. B. A., Worden, J. R., Noone, D., Parrington, M., and Kar, J.: Analysis of the summertime buildup of tropospheric ozone abundances over the Middle East and North Africa as observed by the Tropospheric Emission Spectrometer instrument, J. Geophys. Res., 114, D05304, doi:10.1029/2008JD010993, 2009.

Liu, X., Chance, K., Sioris, C. E., Spurr, R. J. D., Kurosu, T. P., Martin, R. V., and Newchurch, M. J.: Ozone profile and tropospheric ozone retrieval from the Global Ozone Monitoring Experiment: Algorithm description and validation, J. Geophys. Res., 110, D20307, doi:10.1029/2005JD006240, 2005.

Liu, X., Bhartia, P. K., Chance, K., Spurr, R. J. D., and Kurosu, T. P.: Ozone profile retrievals from the Ozone Monitoring Instrument, Atmos. Chem. Phys., 10, 2521–2537, doi:10.5194/acp-10-2521-2010, 2010.

Logan, J. A.: An analysis of ozonesonde data for the troposphere: Recommendations for testing 3-D models and development of a gridded climatology for tropospheric ozone, J. Geophys. Res, 104, 16115–16149, doi:10.1029/1998JD100096, 1999.

Mao H., Talbot, R., Troop, D., Johnson, R., Businger, S., and Thompson, A. M.: Smart balloon observations over the North Atlantic: O_3 data analysis and modeling, J. Geophys. Res., 111, D23S56, doi:10.1029/2005JD006507, 2006.

McConnell, R., Berhane, K., Gilliland, F., London, S. J., Islam, T., Gauderman, W. J., Avol, E., Margolis, H. G., and Peters, J. M.: Asthma in exercising children exposed to ozone: A cohort study, Lancet, 359, 386–391, 2002.

McPeters, R. D., Labow, G. J., and Johnson, B. J.: A satellite-derived ozone climatology for balloonsonde estimation of total column ozone, J. Geophys. Res., 102, 8875–8885, 1997.

McPeters, R. D., Labow, G. J., and Logan, J. A.: Ozone climatological profiles for satellite retrieval algorithms, J. Geophys. Res., 112, D05308, doi:10.1029/2005JD006823, 2007.

McPeters, R. D. and Labow, G. J.: Climatology 2011: An MLS and sonde derived ozone climatology for satellite retrieval algorithms, J. Geophys. Res., 117, D10303, doi:10.1029/2011JD017006, 2012.

Merrill, J., Bleck, R., and Avila, L.: Modeling Atmospheric Transport to the Marshall Islands, J. Geophys. Res., 90, 12927–12936, 1985.

Methven, J., Arnold, S. R., O'Connor, F. M., Barjat, H., Dewey, K., Kent, J., and Brough, N.: Estimating photochemically produced ozone throughout a domain using flight data and a Lagrangian model, J. Geophys. Res., 108, 4271, doi:10.1029/2002JD002955, 2003.

Minschwaner, K., Kalnajs, L. E., Dubey, M. K., Avallone, L. M., Sawaengphokai, P. C., Edens, H. E., and Winn, W. P.: Observation of enhanced ozone in an electrically active storm over Socorro, NM: Implications for ozone production from corona discharges, J. Geophys. Res., 113, D17208, doi:10.1029/2007JD009500, 2008.

Morris, G. A, Gleason, J. F., Ziemke, J., and Schoeberl, M. R.: Trajectory mapping: A tool for validation of trace gas observations, J. Geophys. Res., 105, 17875–17894, 2000.

Morris, G. A., Thompson, A. M., Pickering, K. E., Chen, S., Bucsela, E. J., and Kucera, P. A.: Observations of ozone production in a dissipating tropical convective cell during TC4, Atmos. Chem. Phys., 10, 11189–11208, doi:10.5194/acp-10-11189-2010, 2010.

Morris, G. A., Labow, G., Akimoto, H., Takigawa, M., Fujiwara, M., Hasebe, F., Hirokawa, J., and Koide, T.: On the use of the correction factor with Japanese ozonesonde data, Atmos. Chem. Phys., 13, 1243–1260, doi:10.5194/acp-13-1243-2013, 2013.

Newman, P. A. and Schoeberl, M. R.: A reinterpretation of the data from the NASA Stratosphere-Troposphere Exchange Project, Geophys. Res. Lett., 22, 2501–2504, 1995.

Oltmans, S. J., Lefohn, A. S., Shadwick, D., Harris, J. M., Scheel, H. E., Galbally, I., Tarasick, D. W., Johnson, B. J., Brunke, E.-G., Claude, H., Zeng, G., Nichol, S., Schmidlin, F., Davies, J., Cuevas, E., Redondas, A., Naoe, H., Nakano, T., and Kawasato, T.: Recent Tropospheric Ozone Changes – A Pattern Dominated by Slow or No Growth, Atmos. Environ., 67, 331–351, doi:10.1016/j.atmosenv.2012.10.057, 2012.

Palmer, P. I., Parrington, M., Lee, J. D., Lewis, A. C., Rickard, A. R., Bernath, P. F., Duck, T. J., Waugh, D. L., Tarasick, D. W., Andrews, S., Aruffo, E., Bailey, L. J., Barrett, E., Bauguitte, S. J.-B., Curry, K. R., Di Carlo, P., Chisholm, L., Dan, L., Forster, G., Franklin, J. E., Gibson, M. D., Griffin, D., Helmig, D., Hopkins, J. R., Hopper, J. T., Jenkin, M. E., Kindred, D., Kliever, J., Le Breton, M., Matthiesen, S., Maurice, M., Moller, S., Moore, D. P., Oram, D. E., O'Shea, S. J., Owen, R. C., Pagniello, C. M. L. S., Pawson, S., Percival, C. J., Pierce, J. R., Punjabi, S., Purvis, R. M., Remedios, J. J., Rotermund, K. M., Sakamoto, K. M., da Silva, A. M., Strawbridge, K. B., Strong, K., Taylor, J., Trigwell, R., Tereszchuk, K. A., Walker, K. A., Weaver, D., Whaley, C., and Young, J. C.: Quantifying the impact of BOReal forest fires on Tropospheric oxidants over the Atlantic using Aircraft and Satellites (BORTAS) experiment: design, execution and science overview, Atmos. Chem. Phys., 13, 6239–6261, doi:10.5194/acp-13-6239-2013, 2013.

Parrish, D. D., Law, K. S., Staehelin, J., Derwent, R., Cooper, O. R., Tanimoto, H., Volz-Thomas, A., Gilge, S., Scheel, H.-E., Steinbacher, M., and Chan, E.: Long-term changes in lower tropospheric baseline ozone concentrations at northern mid-latitudes, Atmos. Chem. Phys., 12, 11485–11504, doi:10.5194/acp-12-11485-2012, 2012.

Pierrehumbert, R.: Lateral Mixing as a Source of Subtropical Water Vapor, Geophys. Res. Lett., 25, 151–154, 1998.

Pierrehumbert, R. and Roca, R.: Evidence for Control of Atlantic Subtropical Humidity by Large Scale Advection, Geophys. Res. Lett., 25, 4537–4540, 1998.

Roelofs, G.-J. and Lelieveld, J.: Model study of the influence of cross-tropopause O_3 transports on tropospheric O_3 levels, Tellus, B, 49, 38–55, 1997.

Royal Society: Ground-level ozone in the 21st century: future trends, impacts and policy implications, Science Policy Report 15/08, October 2008, RS1276, (http://royalsociety.org/policy/publications/2008/ground-level-ozone/), 2008.

Sauvage, B., Thouret, V., Cammas, J.-P., Gheusi, F., Athier, G., and Nédélec, P.: Tropospheric ozone over Equatorial Africa: regional aspects from the MOZAIC data, Atmos. Chem. Phys., 5, 311–335, doi:10.5194/acp-5-311-2005, 2005.

Smit, H. G. J. and Straeter, W.: JOSIE-2000, Jülich Ozone Sonde Intercomparison Experiment 2000, The 2000 WMO international intercomparison of operating procedures for ECC-ozonesondes at the environmental simulation facility at Jülich, WMO Global Atmosphere Watch report series, No. 158 (Technical Document No. 1225), World Meteorological Organization, Geneva, 2004.

Smit, H. G. J., Sträter, W., Helten, M., Kley, D., Ciupa, D., Claude, H. J., Köhler, U., Hoegger, B., Levrat, G., Johnson, B., Oltmans, S. J., Kerr, J. B., Tarasick, D. W., Davies, J., Shitamichi, M., Srivastav, S. K., and Vialle, C.: JOSIE: The 1996 WMO international intercomparison of ozonesondes under quasi-flight conditions in the environmental chamber at Jülich, in: Atmospheric Ozone: Proceedings of the Quadrennial O_3, Symposium, l'Aquila, Italy, edited by: Bojkov, R. D. and Visconti, G., 971–974, Parco Sci. e Tecnol. d'Abruzzo, Italy, 1996.

Smit, H. G. J., Straeter, W., Johnson, B., Oltmans, S., Davies, J., Tarasick, D. W., Hoegger, B., Stubi, R., Schmidlin, F., Northam, T., Thompson, A., Witte, J., Boyd, I., and Posny, F.: Assessment of the performance of ECC-ozonesondes under quasi-flight conditions in the environmental simulation chamber: Insights from the Juelich Ozone Sonde Intercomparison Experiment (JOSIE), J. Geophys Res., 112, D19306, doi:10.1029/2006JD007308, 2007.

Stendel, M. and Arpe, K.: Evaluation of the hydrological cycle in reanalyses and observations, Max-Planck-Institute for Meteorology, Report No. 228, 52 pp, available from Max-Planck-Institut

für Meteorologie, Bundesstrasse 55, 20147 Hamburg, Germany, 1997.

Stevenson, D. S., Dentener, F. J., Schultz, M. G., Ellingsen, K., van Noije, T. P. C., Wild, O., Zeng, G., Amann, M., Atherton, C. S., Bell, N., Bergmann, D. J., Bey, I., Butler, T., Cofala, J., Collins, W. J., Derwent, R. G., Doherty, R. M., Drevet, J., Eskes, H. J., Fiore, A. M., Gauss, M., Hauglustaine, D. A., Horowitz, L. W., Isaksen, I. S. A., Krol, M. C., Lamarque, J.-F., Lawrence, M. G., Montanaro, V., Müller, J.-F., Pitari, G., Prather, M. J., Pyle, J. A., Rast, S., Rodriguez, J. M., Sanderson, M. G., Savage, N. H., Shindell, D. T., Strahan, S. E., Sudo, K., and Szopa, S.: (2006), Multimodel ensemble simulations of present-day and near-future tropospheric ozone, J. Geophys. Res., 111, D08301, doi:10.1029/2005JD006338, 2006.

Stohl, A.: Computation, accuracy and applications of trajectories – a review and bibliography, Atmos. Environ., 32, 947–966, 1998.

Stohl, A. and Seibert, P.: Accuracy of trajectories as determined from the conservation of meteorological tracers, Q. J. Roy. Meteor. Soc., 124, 1465–1484, doi:10.1002/qj.49712454907, 1998.

Stohl, A., James, P., Forster, C., Spichtinger, N., Marenco, A., Thouret, V., and Smit, H. G. J.: An extension of Measurement of Ozone and Water Vapour by Airbus In-service Aircraft (MOZAIC) ozone climatologies using trajectory statistics, J. Geophys. Res., 106, 27757–27768, doi:10.1029/2001JD000749, 2001.

Stübi, R., Levrat, G., Hoegger, B., Viatte, P., Staehelin, J., and Schmidlin, F. J.: In-flight comparison of Brewer-Mast and electrochemical concentration cell ozonesondes, J. Geophys. Res., 113, D13302, doi:10.1029/2007JD009091, 2008.

Sutton, R. T., Maclean, H., Swinbank, R., O'Neill, A., and Taylor, F. W.: High-Resolution Stratospheric Tracer Fields Estimated from Satellite Observations Using Lagrangian Trajectory Calculations, J. Atmos. Sci., 51, 2995–3005, 1994.

Tarasick, D. W., Davies, J., Anlauf, K., Watt, M., Steinbrecht, W., and Claude, H. J.: Laboratory investigations of the response of Brewer-Mast sondes to tropospheric ozone, J. Geophys. Res., 107, 4308, doi:10.1029/2001JD001167, 2002.

Tarasick, D. W., Fioletov, V. E., Wardle, D. I., Kerr, J. B., and Davies, J.: Changes in the vertical distribution of ozone over Canada from ozonesondes: 1980–2001, J. Geophys. Res., 110, D02304, doi:10.1029/2004JD004643, 2005.

Tarasick, D. W., Jin, J. J., Fioletov, V. E., Liu, G., Thompson, A. M., Oltmans, S. J., Liu, J., Sioris, C. E., Liu, X., Cooper, O. R., Dann, T., and Thouret, V.: High-resolution tropospheric ozone fields for INTEX and ARCTAS from IONS ozonesondes, J. Geophys. Res., 115, D20301, doi:10.1029/2009JD012918, 2010.

Tilmes, S., Lamarque, J.-F., Emmons, L. K., Conley, A., Schultz, M. G., Saunois, M., Thouret, V., Thompson, A. M., Oltmans, S. J., Johnson, B., and Tarasick, D.: Technical Note: Ozonesonde climatology between 1995 and 2011: description, evaluation and applications, Atmos. Chem. Phys., 12, 7475–7497, doi:10.5194/acp-12-7475-2012, 2012.

von Kuhlmann, R., Lawrence, M. G., Crutzen, P. J., and Rasch, P. J.: A model for studies of tropospheric ozone and nonmethane hydrocarbons: Model description and ozone results, J. Geophys. Res., 108, 4294, doi:10.1029/2002JD002893, 2003.

Worden, H. M., Logan, J. A., Worden, J. R., Beer, R., Bowman, K., Clough, S. A., Eldering, A., Fisher, B. M., Gunson, M. R., Herman, R. L., Kulawik, S. S., Lampel, M. C., Luo, M., Megretskaia, I. A., Osterman, G. B., and Shephard, M. W.: Comparisons of Tropospheric Emission Spectrometer (TES) ozone profiles to ozonesondes: Methods and initial results, J. Geophys. Res., 112, D03309, doi:10.1029/2006JD007258, 2007a.

Worden, J., Liu, X., Bowman, K., Chance, K., Beer, R., Eldering, A., Gunson, M., and Worden, H.: Improved tropospheric ozone profile retrievals using OMI and TES radiances, Geophys. Res. Lett., 34, L01809, doi:10.1029/2006GL027806, 2007b.

World Climate Research Programme, SPARC/IOC/GAW Assessment of Trends in the Vertical Distribution of Ozone, Stratospheric Processes and Their Role in Climate, World Meteorol. Organ. Global Ozone Res. Monit. Proj. Rep, 43, Geneva, Switzerland, 1998.

World Meteorological Organization, International meteorological vocabulary, WMO Rep. 182, World Meteorol. Org., Geneva, Switzerland, 1992.

Young, P. J., Archibald, A. T., Bowman, K. W., Lamarque, J.-F., Naik, V., Stevenson, D. S., Tilmes, S., Voulgarakis, A., Wild, O., Bergmann, D., Cameron-Smith, P., Cionni, I., Collins, W. J., Dalsøren, S. B., Doherty, R. M., Eyring, V., Faluvegi, G., Horowitz, L. W., Josse, B., Lee, Y. H., MacKenzie, I. A., Nagashima, T., Plummer, D. A., Righi, M., Rumbold, S. T., Skeie, R. B., Shindell, D. T., Strode, S. A., Sudo, K., Szopa, S., and Zeng, G.: Preindustrial to end 21st century projections of tropospheric ozone from the Atmospheric Chemistry and Climate Model Intercomparison Project (ACCMIP), Atmos. Chem. Phys., 13, 2063–2090, doi:10.5194/acp-13-2063-2013, 2013.

Ziemke, J. R., Chandra, S., Duncan, B. N., Froidevaux, L., Bhartia, P. K., Levelt, P. F., and Waters, J. W.: Tropospheric ozone determined from Aura OMI and MLS: Evaluation of measurements and comparison with the Global Modeling Initiative's Chemical Transport Model, J. Geophys. Res., 111, D19303, doi:10.1029/2006JD007089, 2006.